Development and Application of Human Skeletal Muscle Microphysiological Systems

George A. Truskey[a]

[a.]Department of Biomedical Engineering, Duke University, 1425 CIEMAS, 101 Science Drive, Durham, NC 27708-0281; Tel: 919-660-5147; gtruskey@duke.edu

Abstract

A number of major disease states involve skeletal muscle, including type 2 diabetes, muscular dystrophy, sarcopenia and cachexia arising from cancer or heart disease. Animals do not accurately represent many of these disease states. Human skeletal muscle microphysiological systems derived from primary or induced pluripotent stem cells (hPSCs) can provide an *in vitro* model of genetic and chronic diseases and assess individual variations. Three-dimensional culture systems more accurately represent skeletal muscle function than do two-dimensional cultures. While muscle biopsies enable culture of primary muscle cells, hPSCs provide the opportunity to sample a wider population of donors. Recent advances to promote maturation of PSC-derived skeletal muscle provide an alternative to primary cells. While contractile function is often measured in three-dimensional cultures and several systems exist to characterize contraction of small numbers of muscle fibers, there is a need for functional measures of metabolism suited for microphysiological systems. Future research should address generation of well-differentiated hPSC-derived muscle cells, enabling muscle repair *in vitro*, and improved disease models.

Introduction

Skeletal muscle accounts for 40% of body weight and is one of the most metabolically active tissues, adapting energy sources depending on the type and duration of activity. Muscle consumes 30% of the body's energy under resting conditions and as much as 80% under strenuous exercise. Skeletal muscle accounts for 75% of insulin-stimulated glucose metabolism and much of the glucose is stored as glycogen[1]. Muscle function is altered by disease, disuse, and injury. Diseases that affect skeletal muscle, including those affecting motor neurons, alter mobility and key body functions such as respiration[2]. Examples include muscular dystrophy[2] and myasthenia gravis[3]. In the elderly, loss of muscle mass and function (sarcopenia) is major cause of falls, which often have severe effects on morbidity and mortality among the elderly[4]. Metabolic diseases, such as type 2 diabetes, affect energy production and glucose homeostasis in muscle, causing systemic injury[5].

While animal models are used to model disease states and develop treatments, animal models suffer from several limitations. In many cases, a transgenic mouse may be the only

pre-clinical model. However, a transgenic mouse model often does not match the severity or phenotype of human disease or share the same genetic basis, e.g., Duchenne Muscular Dystrophy[6]. For more complex diseases (e.g., cachexia and sarcopenia), mouse genetic knockouts can examine only one or two pathways at a time[7], providing a limited understanding of the disease. While the mouse is widely used in many pre-clinical studies, rodent physiology is drastically different from that in humans and other large animals. For example, humans and mice exhibit drastically different transcriptional responses to inflammatory diseases and variations among mouse strains are significant and unrelated[8].

Advances in methods to produce differentiated cells and tissues from embryonic or induced human pluripotent stem cells (hPSCs) or to transdifferentiate cells, such as fibroblasts to skeletal muscle cells, offer new opportunities to develop *in vitro* disease models to study mechanisms and develop new therapies. To effectively use differentiated cells from individuals with specific diseases, the *in vitro* environment must adequately model *in vivo* conditions. Even when different cell types present in a tissue are cultured together, two-dimensional (2D) cell culture methods are inadequate to model the complex interactions occurring in a tissue or organ, due to spatial organization and the rigidity of tissue culture plastic. More recently, tissue engineering approaches have been used to develop three-dimensional (3D) human microphysiological systems that mimic the key structural and functional features of a tissue or organ. These systems produce functions observed *in vivo* but not in 2D culture.

This review covers the different approaches to generate microphysiological systems for skeletal muscle, the current state of development of hPSC-derived skeletal muscle and how these approaches are used to model human diseases *in vitro*. We note key features of the diseases that need to be modelled and highlight challenges that need to be addressed to develop effective models of human disease *in vitro*.

Approaches to Produce Skeletal Muscle Microphysiological Systems

Primary human or animal myogenic cells for engineered tissues are derived from quiescent satellite cells positive for the transcription factor Pax7[9]. These cells normally reside between the myofiber basal lamina and the sarcolemma and, after injury, proliferate and differentiate to myoblasts. These myoblasts fuse with injured muscle fibers, eliciting repair and a functional muscle fiber. Large numbers of myogenic cells are obtained from biopsies by stimulating these satellite cells to proliferate while limiting the growth of other cells types (e.g. fibroblasts) through a combination of culture on extracellular matrix proteins (e.g. collagen I, laminin, or Matrigel) and media containing high levels of growth factors or serum[10]. Fusion of myoblasts to form myotubes in 2D cultures or tissue-engineered constructs is promoted by reducing the growth factors[11], serum levels, or using serum-free media[12].

Contractile force is an important functional measure for skeletal muscle which can be induced *in vitro* by application of electrical stimulation. Different methods of measuring contractile force have influenced the design of microphysiological systems for skeletal muscle. These systems can be divided into the following groups (1) Three-dimensional

myobundles attached to fixed ends, (2) aligned muscle myotubes attached to deformable posts, and (3) myotubes adherent to materials that directly measure force (Table 1 and Figure 1).

Three-Dimensional Myobundles Attached to Fixed Ends

Myobundles were originally developed by Vandenburgh et al.[13] and consist of multinucleated myotubes usually within hydrogels attached to fixed frames, Velcro, posts, or thin sutures (Fig. 1A). Fibrin and collagen are common biological hydrogels used to fabricate myobundles[10, 14,15]. Compaction induced by myotubes and fibroblasts generates tension between the fixed ends of the myobundle, causing the myotubes to align during formation. The cultures contain some fibroblasts which synthesize extracellular matrix and produce contraction, ensuring stable 3D constructs[16]. Without fibroblasts, the 3D tissue-engineered constructs do not compact and force generation is minimal[16].

Alternatively, sheets of myogenic cells and fibroblasts can be rolled to form 3D structures without a scaffold. This approach results in greatly reduced extracellular matrix, although theses myobundles tend to generate smaller contractile forces[16, 17]. Fibroblasts are essential to produce sufficient force and extracellular matrix in the scaffold-free engineered tissues, possibly synthesizing extracellular matrix and producing lateral linkages with the extracellular matrix[16].

A range of biomaterials have been considered for skeletal muscle tissue engineering applications in which the satellite cell population is implanted into injured muscle for reconstruction and the biomaterial degrades or releases cells[18]. Encapsulating the myoblasts maintains the cells in the wounded area leading to greater repair.

In vitro systems have more stringent requirements for long-term differentiation and maturation of muscle. Muscle stem cell proliferation and self-renewal is improved [19] and skeletal muscle differentiation is optimal[20] on surfaces that have an elastic modulus (12 kPa) similar to that of skeletal muscle[20], whereas the extensional modulus must be stiff enough to resist the contractile forces produced by contracting myotubes and fibroblasts in the myobundles[21]. The hydrogel composition may affect interactions with cell surface integrins and the dystrophin complex, since myotubes don't express α_2 which binds to collagen whereas myotubes express α_7 which binds to laminin synthesized by myotubes and α_V integrin which binds to fibrin[21]. Further, engagement of α_V and α_7 integrins with their ligands activates signaling pathways to promote myotube formation and differentiation. Although collagen occurs in skeletal muscle tissue *in vivo*, collagen gels do not yield aligned fibrils found *in vivo*. As a result, fibrin appears to function better as a hydrogel for skeletal myoblasts, promoting myotubes maturation and resisting failure under higher contraction forces[21].

Given the lot-to-lot variability of biological hydrogels, a synthetic hydrogel is preferable. PEG–maleimide (PEG–MAL) hydrogels incorporating the RGD integrin binding sequence of fibronectin promote myoblast fusion and myotubes alignment and contraction, but maturation is limited and the mechanical properties need to be adjusted to more closely match those of native muscle (17 kPa)[22]. Gelatin-methacrylate (GelMA) hydrogels (5%-7%

v/v) support skeletal myotube formation and alignment[23]. Adding aligned carbon nanotubes to the GelMA promotes myotube alignment and improves the effectiveness of electrical stimulation of myobundles[23]. The elastic modulus of GelMA gels is between 7–12 kPa[23, 24], while the aligned GelMA with aligned carbon nanotubes has a modulus of 20 kPa[23], very close to the value of native muscle. These limited results do suggest that producing a synthetic extracellular matrix for myotubes formation and maturation is feasible, although binding sites to additional integrins important in myoblast differentiation should be incorporated into the biomaterials.

Functional myobundles have been created with the murine cell line C_2C_{12}[21, 25–27], primary avian myogenic cells [13], primary mouse [16, 28] and rat[13, 16, 21] myogenic cells, and human myogenic cells[29–31]. Human skeletal muscle myoblasts from commercial sources appear to function as well as those derived directly from biopsy samples or discarded tissue[31]. The formation of myotubes occurs in a two-step process. Myobundles are first cultured in growth media to increase cell number, then switched to a low serum or serum-free differentiation media to promote myotube formation. Compaction of the hydrogel by the myoblasts and fibroblasts generates traction stresses within the bundle since the ends are fixed (Fig. 1A). As a result, myotubes align in the direction of stress (Fig. 2A). Myobundle lengths range between 0.4–2 cm[17, 32]. Oxygen transport becomes a significant limiting factor for myobundles thicker than about 500 μm and leads to localization of myoblasts and myotubes at the outer rim of the myobundles [25, 33]. For typical initial cell densities (2–20×10^6 cells/mL)[31, 34] and assuming a cylindrical shape, myobundle diameters should be less than 800 μm in diameter to avoid oxygen transport limitations[25, 35].

Since the 3D engineered muscle bundles are attached to fixed points, application of electrical stimulation produces isometric contraction. Passive and active forces have been measured with commercial force transducers and twitch and tetanus forces range from 0.5–2.5 mN depending on cell density, source of cells and extent of maturation (Fig. 2B, C). (The lower limit of sensitivity of current force transducers is ~50 μN.) In particular, the use of dynamic culture in which the culture media is mixed by placing myobundles made with primary newborn rat myocytes on a rocker, produces specific forces (force/area) as high as 40 mN/mm^2 corresponding to a single fiber tetanus force of 8.3±1.0 μN[33]. These specific forces are similar to specific forces for neonate rat muscle[36]. Further, by maintaining a tetanic contraction, the fatigue can be determined by measuring the reduction contractile force after a specified time, providing a sensitive measure of the muscle's ability to meet energetic demands[37].

For myobundles made with human cells, the maximum specific force is about 2 mN/mm^2 (or kPa) for twitch forces and 7 mN/mm^2 for tetanus[31]. The values are close to specific forces for tetanus of human fetal muscle and about 10–20 less than values for adult muscle[38, 39].

Calcium plays a critical role in in regulating skeletal muscle contraction and measurement of calcium dynamics can provide insight into the function of engineered skeletal muscle. Seven days after implantation of engineered skeletal muscle myobundles with primary rat myogenic cells transduced with the calcium reporter GCaMP3, calcium transients were

observed coincident with twitch and tetanus responses[40]. *In vitro*, the normalized change in calcium reporter GCaMP6 fluorescence intensity (F/F) is proportional to the magnitude of the applied force[31], suggesting that the dynamic response of the force provides information on calcium dynamics.

While myobundles made by embedding myoblasts in fibrin hydrogels produce the highest specific forces recorded *in vitro* relative to other fabrication methods, and can reproduce many structural features, they do have several limitations. The extracellular matrix is a greater fraction of the engineered myobundle volume (40%-50%) than skeletal muscle tissue *in vivo* (5%). This is particularly true for rodent myobundles in which the initial cell density is 2.5–7.5×10^6 cells/mL for rodent cells [34] and 15×10^6 cells/mL for human cells[31]. Increasing the initial cell density to 15×10^6 cells/mL and increasing cell mixing produced a 40% volume fraction of myotubes and myogenic cells and led to significant increases in the contractile force[33]. As noted, the extracellular matrix proteins are needed to produce high contractile forces since engineered muscle prepared without extracellular matrix proteins or hydrogels (termed myooids) produce lower specific forces than myobundles[17].

A novel microfluidic device that reduced the size of the myobundles (Fig. 1B) consists of an inner hairpin microchannel for the skeletal muscle collagen gel myobundles to form and an outer hairpin channel for the culture media[41]. Media exchange between the two channels occurred via small interconnecting microchannels. Posts at the entrance and exit of the cell microchannel enabled tension to develop as the collagen gel with cells compacted. After 6 days of culture the collagen gel had compacted to a region less than 100 μM thick. The displacement of the myobundle following a single 1 Hz and 50 Hz stimuli resemble what would be expected for twitch and tetanus. Further work is needed to optimize this system and measure forces. This system may prove for higher throughput drug screening and study of metabolic conditions.

Myotubes Attached to Deformable Microposts

Microscale cardiac and skeletal muscle engineered tissues have been produced by either self-assembly of cells around two polymeric posts or by addition of the cells to a hydrogel that polymerizes around and between the posts (Fig. 1C). The posts have a length L, radius a, and elastic modulus E. When the bundle contracts due to passive or active forces, the posts bend. The deflection of the posts (δ) of length L and width a arises from passive contractile forces of the myobundle plus any added active force generation. As long as the deflection is small relative to the beam length, then beam theory[42] can be applied to calculate the force (F) generated by the myobundle is $F = 3\pi Ea^4\delta/4L^3$, where E is the elastic modulus of the posts. The forces produced are often validated with a force sensor or calibrated cantilevers[42]. The posts are separated by distances ranging from 300 μm[43] to 4000 μm[32].

The elastic modulus of the skeletal muscle microtissues derived from the C2C12 mouse myoblast line is about 12 kPa[43], similar to the modulus of C2C12 cells during early stages of differentiation in 2D culture on rigid substrates [44]. While the strains in the myobundles after formation are uniform, compaction results in nonuniform strains concentrated around the microposts[45]. Twitch and tetanus forces can be examined and fatigue can be induced by maintaining a fixed electrical stimulation to induce tetanus for prolonged times. Forces as

low as 2–4 µN can be reliably measured from a few hundred cells added initially to the microtissue [42]. Given the scale of the posts, these systems can be placed in a 48 well format for moderate throughput for drug screening [32]. Advantages of this approach are the small numbers of cells that can be used, the ability to track the active and passive force of a single microtissue over time, assessment of the response to drugs and the small number of cells needed to establish the system. The dynamic response of these systems to report twitch kinetics has not been reported.

Most skeletal muscle microphysiological systems use electrical stimulation to depolarize the cell membrane, releasing calcium from the sarcoplasmic reticulum and initiating contraction. Prolonged electrical stimulation can promote maturation of the skeletal muscle myofibers and increased myobundle force production [46]. While this approach mimics the key feature of membrane depolarization to initiate contraction, the electric fields produced can damage the muscle by electroporation [46] or oxidation of the culture media[47], even when stimulation is biphasic. Thus, frequent media changes are needed to minimize damage to the engineered muscle tissue.

An alternative approach to initiate contraction has been to express channelrhodopsin-2 (ChR2) in the myoblasts, followed by optical stimulation to induce contraction of skeletal myotubes in 2D [43, 48] or 3D myobundles [43]. The extent of contraction of individual myotubes is similar for optical and electrical stimulation [48]. The contractile force of thick muscle strips (1,200 µm) is smaller when optically stimulated than when electrically stimulated[43, 49]. The force produced by optical stimulation increases when the myobundle thickness decreases to about 700 µm or the light intensity increases, suggesting that the more muscle fibers are stimulated[49]. Regular optical stimulation of the optically active myobundle rings causes alignment of the myofibers and increases the contractile force[49]. Limitations of the system are that force-length relations cannot be obtained and the extent of differentiation remains to be validated.

Optical stimulation facilitates generation of bio-based micromachines. Thin rings of engineered muscle with optogenetically modified skeletal muscle can be fashioned to mechanical supports and the stimulated to produce directed motion[49]. By patterning the orientation of optically stimulated cardiomyocytes to a PDMS membrane, optically stimulation was used to generate motion similar to that of a stingray[50].

Myotubes adherent to materials that directly measure force

In these systems, thin films made with polydimethylsiloxane (PDMS)[51] or other polymers, or silicon coated cantilevers[52] are modified to allow muscle cell growth and fusion to form myotubes. Electrical stimulation to contract myotubes causes the PDMS film to curve. Micropatterning of the material is necessary to enable the myotubes to align[53].

The passive and active stress exerted by these muscular thin films[53] is computed using the curvature, elastic modulus of the PDMS and thickness of the polymer and cell layers[51] (Fig. 1D). The effect of different regimes of electrical stimulation can be examined and the systems can be multiplexed to analyze up to 35 muscular thin films on a single chip and chips can be perfused to perform dose-response studies[54]. A recently developed

photopatterning approach to produce gelatin films should facilitate the development of high throughput platforms to examine drug toxicity and efficacy[55].

The cantilever systems, like the thin films, consist of a single layer of cells adherent to the cantilever (Fig. 1E). Stresses exerted by the myotube layer induces a deflection of the cantilever that alters the path of a laser that is measured by a photodetector[52]. The force is determined from cantilever beam bending model using a modified Stoney's equation[52]. Cantilevers are typically 750 μm long and 100 μm wide enabling long myotubes to form. Forces as low as 20 nN can be measured[56], representing a few myotubes. Twitch forces and fatigues can be measured[57]. Given the small size of the cantilevers, the system is amenable to high throughput screening[57].

A limitation of these systems is that the cells form a single layer on PDMS or cantilever, so the systems are inherently 2D. Further, the muscle tissue cannot be stretched and force-length relationships cannot be obtained.

Differentiation of Skeletal Muscle from hPS Cells or Other Cell Types

While myogenic cells can be obtained from muscle biopsies, such biopsies are often challenging for individuals with a number of muscle diseases, such as muscular dystrophy. Further, the isolated cells last for a limited period before senescence or dedifferentiation. Alternatively, differentiating skeletal muscle cells from hPSCs provides a continuous source of cells from individual donors. Several protocols have been developed that yield both Pax7+ cells and myoblasts from hPSCs[58–61], as reviewed recently[62]. While these differentiated cells can be used for one or a few passages, new stocks of differentiated can be continuously regenerated without having to sample the patient. Induced expression of Pax7 in hPSCs leads to improved formation of myotubes in myobundles attached to deformable posts[59]. Expandable myogenic progenitors, termed induced myogenic progenitor cells (iMPCs), were produced followed by inducible expression of satellite cell marker Pax7 (Fig. 3)[58]. hPSC-derived iMPCs were capable of highly efficient 2D differentiation *in vitro*, yielding both functional myotubes and resident Pax7$^+$ cells, the two main constituents of native skeletal muscle[58]. By 2 weeks of differentiation, iMPCs readily fused into spontaneously contracting, multinucleated myotubes (7–10 nuclei), expressing MyoG, acetylcholine (ACh) receptors, and the muscle-specific structural protein sarcomeric α-actinin (SAA) arranged in a cross-striated pattern. These hPS-derived skeletal myoblasts (iSKM) were used to prepare 3D myobundles. At 2 weeks of differentiation, iSKM bundles contained densely packed, aligned, cross-striated myotubes that ubiquitously expressed membrane-localized dystrophin and ACh receptors, and were embedded in a laminin and collagen I rich matrix[58]. Similar to primary human myobundles, iSKM bundles showed twitch and tetanic contractions, and a positive force–frequency relationship in response to electrical stimulation. Passive tension and twitch kinetics of iSKM bundles remained stable during 4-week culture and similar in magnitude to that of primary human myobundles[58].

An alternative approach to produce skeletal muscle has been by forced overexpression of MyoD, one of several early transcription factors in myogenesis[63]. After MyoD overexpression, a subset of fibroblasts undergo fusion and produce striated myotubes[63].

However, MyoD activates a subset of genes in fibroblasts needed for complete differentiation to myoblasts and myotubes, and is limited by chromatin sites not accessible to MyoD[64]. By addition of small molecules that activate or inhibit specific signaling pathways, MyoD-induced differentiation of fibroblasts was enhanced by blocking TGFα and activin pathways or activation of canonical WNT signaling[65]. Alternatively, expression of MYD and MYCL enhanced expression of muscle genes for myogenin, creatine kinase and dystrophin and promoted fusion of myotubes[66]. MYCL may act by suppressing fibroblast-specific genes[66]. 3D engineered myobundles have not yet been produced by transdifferentiation of fibroblasts, so the potential of this approach is not fully known.

Innervation of Skeletal Muscle Microphysiological Systems

Most *in vitro* engineered 3D muscle systems lack innervation. *In vivo*, denervation causes loss of muscle mass, a decrease in type 2 fibers, disorganization of sarcomeres and decreased contraction speed. These effects can be reversed partially by electrical stimulation of myobundles[67]. Alternatively, treatment of myobundles with miniagrin, a recombinant C-terminal fragment of agrin, which is secreted by nerves and promotes muscle maturation, increased twitch and tetanus force, promoted acetylcholine receptor clusters and dystrophin gene expression[68], suggesting that neurotrophic factors can improve skeletal muscle function.

Adding neural cells to myooid cultures derived from fetal rat skeletal myoblasts resulted in the formation of neuromuscular-like junctions and significant increases in twitch (2X) and tetanus (1.7X) forces relative to myooids without neurons[69]. Likewise, myobundles prepared with rat primary myogenic cells and embryonic rat motor neurons formed structures resembling neuromuscular junctions[70]. Chemical stimulation of neurons with glutamate induced myobundle contraction[71] and blocking the acetylcholine receptor with d-tubocurarine inhibits spontaneous neural stimulation of myobundle contraction[70]. Twitch and tetanus force were increased and fetal forms of myosin heavy chain decreased when the neuromuscular junction was stimulated[70]. Similar results have been obtained using innervated myotubes adherent to cantilever beams to record force[72], although only a small fraction of skeletal muscle on cantilevers were innervated. Thus, incorporation of motor neurons may more closely model the *in vivo* muscle structure. A limitation of these systems is that individual neurons are not stimulated, but depolarization of all neurons occurs with electrodes placed in the culture media.

A multicompartment microfluidic device for neuron cultures[73] has been adapted to produce neuromuscular junctions. Neurons cell bodies are separated from other cell types by narrow parallel mircogrooves through which axons extend [73] (Fig. 4). The system enables long-term culture of neurons and facilitates microscopy and RNA isolation. Formation of myotubes in the second compartment accelerates axonal extension from the neuron compartment leading to formation of formation of neuromuscular junction in both 2D cultures and 3D myobundle systems. A similar design was used to create neuromuscular junctions of human muscle myotubes and hPS-derived neurons that demonstrated tetanus and exhibited inhibition in the response of the myotubes to neurotoxins[74]. This system now makes possible the *in vitro* study of a variety of neuromuscular diseases.

The multi-compartment neural culture system has been extended to culture myobundles attached to deformable posts in the central compartment[75] (Fig. 5). Optogenetic probes were inserted in both the motor neurons derived from mouse embryonic stem cells and the skeletal muscle and 3D muscle contraction was induced by optical stimulation of neurons. The advantage of this approach is that neurons can be selectively stimulated, mimicking *in vivo* conditions. The forces generated by optical stimulation were 70% of those generated by electrical simulation and optical stimulation of neurons was unable to induce tetanus[75], suggesting incomplete innervation of the myobundle. While further work is needed to develop neuromuscular junctions, this system offers an important approach to develop a true biomimetic system and promote further skeletal muscle differentiation.

Application of Skeletal Muscle Microphysiological Models for Muscle Function and Drug Toxicity Assessment

Skeletal Muscle Metabolism

Microphysiological systems represent important tools to examine factors that affect normal tissue function by constructing minimal systems and then adding levels of complexity. The influence of various biochemical and biophysical stimuli can be examined under more realistic conditions than can be produced with 2D systems. As an example, these 3D systems have demonstrated the importance of using hydrogels to match the elastic properties of tissue promotes differentiation as long as the myoblasts and myotubes can interact with the hydrogel via integrins[21]. While considerable effort has focused upon optimizing force generation by myobundles, much less attention has been given to the metabolic state of myobundles *in vitro*.

Cultured myotubes from cell lines and primary cells exhibit a much less robust increase in insulin-stimulated glucose uptake compared to skeletal muscle *in vivo*[76–83], along with elevated levels of constitutive (GLUT1) glucose transporters relative to insulin-sensitive (GLUT4) glucose transporters [78, 84]. In engineered myooids made with primary rat myoblasts, glucose uptake was 5–6 times higher than it was for rat soleus muscle, due largely to an 8-fold increase in the constitutive glucose transporter GLUT1[85]. Due to extensive basal uptake by GLUT1, insulin-mediated glucose uptake increased only 40% relative to basal glucose levels[85], whereas *in vivo* insulin-mediated glucose uptake in muscle is about 6–8 times above basal levels.

Culture conditions influence the level of glucose uptake and expression of GLUT1 and GLUT4. Myobundles cultured in high glucose (25 mM) media exhibit higher levels of GLUT4 and phosphofructokinase, which may be indicative of a more glycolytic phenotype [86]. Insulin may promote growth of myoblasts[31], but chronic exposure to 100 nM insulin increases basal levels of glucose uptake and abolishes the effect of exogenous insulin addition by suppressing GLUT4 levels[87]. Interestingly, measurements of intrinsic NADH and FAD intrinsic fluorescence suggest that myotubes in 3D bundles may be more metabolically active than myotubes in 2D culture[88].

Skeletal muscle *in vivo* can be classified as fast or slow based on oxidative versus glycolytic metabolism and the presence of myosin heavy chain (MHC) isoforms[89]. Myobundles prepared from rat soleus (96% Type I slow muscle fibers)[90] and rat tibialis anterior (14% Type I, 30% Type IIa, 25.2 Type IIX))[90] exhibited differences in force, fatigue, calcium handling and MHC isoform expression consistent with the tissue of origin[91]. In the mouse, however, the soleus exhibits a lower fraction of type I fibers (31% Type I, 51% IIa, 15% IIx, and 3% IIb)[90] and tibialis anterior is predominately type II (0.6% Type I 18.2% IIa, 44.7% IIX)[90]. Consistent with the dominant fiber type, myobundles prepared with myoblasts from the mouse soleus had better fatigue resistance and lower amounts of the glycolytic protein phosphofructokinase and more of oxidative proteins than myobundles prepared with myoblasts from the mouse tibialis anterior[28]. These results suggest that myoblasts appear to retain memory of the fiber type and other epigenetic changes after isolation *in vitro*.

Culture conditions can cause modest shifts in muscle phenotype. Chronic low frequency electrical stimulation for two weeks (0.6 s stimulation at 10–20 Hz followed by 0.4 s rest) produces an oxidative phenotype with elevated GLUT4, increased fatigue resistance, increased levels of mitochondrial enzymes for oxidative metabolism and reduced fast MHC protein levels[27] and protein levels of phosphofructokinase, the rate-limiting enzyme in glycolysis[15]. Culturing the myobundles in low glucose[86] or addition of microRNAs that promote skeletal muscle differentiation [92] can cause modest shifts towards the slow muscle phenotype. Addition of static strain promotes skeletal myotube differentiation and hypertrophy,[93] and may potentially influence fiber type, particularly when coupled with electrical stimulation and changes in media composition.

Drug Responses

Given the increasing cost to develop new drugs, limitations of animal models to replicate many disease states, and the high failure rates in clinical trials, there is considerable interest in developing new approaches to identify the most promising drug candidates. High throughput screening assays were developing using a single molecular target. While gene and protein expression assays are helpful to characterize the general state of the cell, functional assays of one or more important physiological variables indicate the overall state of the tissue or organ[94].

A number of drugs are toxic to skeletal muscle. Toxicity can range from muscle pain and weakness to more significant problems such as muscle inflammation (myositis) and muscle death. Muscle injury and death causes release of creatine kinase and other muscle proteins into blood. Rapid and massive muscle death can lead to kidney failure and death, a condition known as rhabdomylosis. Myopathies that can lead to rhabdomylosis have been caused by a number of drugs including the statin, cerivastatin [95], as well as certain immunosuppressive drugs (cyclosporine, tacrolimus) and drugs that adversely affect mitochondria[96].

Several studies have demonstrated the ability of 3D myobundles to replicate key responses to drugs. Myobundles made with primary mouse myoblasts attached to deformable posts and exposed to 2.5 μM atorvastatin for 2 days or 0.01 μM atorvastatin for 3 days showed a significant reduction in contractile force and evidence of cell death. In contrast, myobundles made with human myoblasts from 2 of 3 donors tolerated pharmacological doses of

lovastatin (0.2 μM), but exhibited reduced force production after exposure to 2.5 μM [31]. In contrast, exposure of human myobundles to 0.05 μM cerivastatin for 2 weeks reduced contractile force by at least 50% and led to lipid accumulation[31]. Human myobundles also exhibited expected dose-dependent toxicity to the anti-malarial drug chloroquine, whereas as low doses of clenbuterol below 1 μM increased force production relative to untreated muscle due to hypertrophy, but decreased contractile function at higher doses [31]. Human myobundles exhibited toxicity following a 24 h exposure to 10 μM terfenadine, as exhibited by reduced contractile forces (Fig. 6), although at higher doses (10 μM) than those which cause toxicity to cardiac muscle by blocking the potassium channel hERG (K_I= 10 nM) causing arrhythmia[97]. The lower toxicity of terfenadine is consistent with the lower affinity for the human eag2 potassium channel present in skeletal muscle and brain[98]. By functionally integrating human skeletal muscle myobundles with a liver system, terfenadine is metabolized to the biologically active form fexofenadine[99], preventing a decline in force. By preparing myobundles in series with an elastic membrane with embedded microparticles that serves as a force transducer (Fig. 7), the time course of passive and active forces of individual myobundles in response to drug treatment can be followed, enhancing sensitivity[100].

Oxygen metabolism influences force production. Rotenone is a pesticide, insecticide, and pisicide that inhibits mitochondrial complex 1. Oxygen consumption of human myobundles was inhibited by 50% at 9 nM rotenone[35]. Myobundle fatigue was more sensitive than twitch or tetanus force to rotenone and oxygen consumption was inversely related to fatigue[35].

Developing disease Model using Skeletal Muscle Microphysiological Systems

Developing improved *in vitro* disease models involves replicating tissue organization using multiple cell types in a 3D environment with media conditions that promote the differentiated state found in tissues, use of cells-derived from individuals that have the disease, and/or creating the microenvironment that infectious diseases exploit [101]. Activation of specific signaling pathways and subsequent cellular responses are dependent on the local environment [102]; consequently, the response to a drug changes depending on the state of the cells (e.g. quiescent, inflammatory) [102]. To date, only a few disease states have been published that use engineered skeletal muscle myobundles.

Atrophy

Skeletal muscle atrophy can arise from prolonged bedrest or limb immobilization after injury, illness among the elderly, neuromuscular disease, or prolonged spaceflight. In a mouse cell myobundle model, atrophy was modeled by reducing the tension on myobundles by reducing the myobundle length by 25% to 50% for 6 days[34]. This change reduced the tetanic force by 50%, reduced protein synthesis rates and decreased myotube cross-sectional area, but did not affect protein degradation rates[34]. In contrast, removal of the tension of the bundle often leads to cell death, suggesting that length reduction may be a very useful *in vitro* model to simulate atrophy while retaining some tension on the myobundles.

Since the glucocorticoid dexamethasone causes muscle atrophy in animal models[103], adding 50–200 μM dexamethasone for 24–48 h reduced the contractile force in myobundles made with C2C12 cells[104], although low doses (e.g. 1 μM) promote myoblast growth *in vitro*[31, 58, 105]. One effect of glucocorticoids is to enhance protein catabolism, and dexamethasone treatment increased levels of the ubiquitin ligases atrogin-1, which regulates MyoD levels, and MURF-1, which regulates myosin heavy chain and actin [104]. Addition of IGF-1, which promotes myoblast growth partially inhibited the effect of dexamethasone and reduced atrogin-1 and MURF-1 levels[104].

Muscular Dystrophy

Muscular dystrophy represents a class of genetic diseases that cause cardiac and skeletal muscle wasting. The most common form is the X-chromosome linked Duchenne muscular dystrophy (DMD) and symptoms appear in the first decade of life[106]. Dystrophin is a critical transmembrane protein that enable muscle to withstand the constant stresses due to muscle motion. The disease is due to several different mutations that delete sections of the protein due deletions of exons[107]. While there are mouse and large animal models to study the disease[107], the symptoms differ from those in humans and *in vitro* human models of the disease could accelerate the development of novel antisense and CRISPR/Cas 9 therapies.

One challenge in testing therapies has been to culture muscle cells from muscular dystrophy patients[108]. Biopsies are feasible, but challenging for individuals with severe muscle diseases. The rarity of disease further limits access to donors. As a result, studies using 3D myobundle models have been limited to one or a few donors[109]. Nonetheless, these models do show that myobundles from muscular dystrophy patients generate lower contractile forces, exhibit misalignment of myotubes along the direction of tension, and thinner myotube diameter[109].

iPS cells have been produced from skin cells of donors with Duchenne's muscular dystrophy and other muscle disease, facilitating studies for the identification of therapies[59]. Even reprogramming fibroblasts with MYOD alone may be sufficient to develop a rapid and high throughput screen [110]. A 3D muscle myobundle using human iPS-derived cardiomyocytes in a ring configuration around deformable posts was used as a functional test to screen for a gene editing approach to correct the disease [108]. Combined with structural measurements, this can be a powerful approach to develop novel gene therapies to treat muscular diseases.

Summary and Perspectives

A number of exciting technologies have been developed to create *in vitro* models of skeletal muscle cells and study diseases. To realize the potential of microphysiological systems, engineering approaches need to be closely integrated with development of robust biological techniques to culture cells. The generation of hPSCs provides a ready source of cells, and a number of proof of principle studies have established that *in vitro* human muscle models so the technology of microphysiological systems can be a valuable approach to study muscle function, and identify treatments for disease. However, the muscle cells produced are still immature, displaying many fetal and perinatal isoforms of muscle proteins, although the adult forms increase in relative amount as the myobundles mature[111]. Several additional

advances are needed before this technology is mature enough to accelerate the discovery of new therapies.

More systematic manipulation of media conditions are needed to optimize growth and differentiation of skeletal muscle *in vitro* and reduce potential damage due to a highly oxidative environment. Some serum-free media formulations have been developed, but there has been limited evaluation as to whether such media is optimally configured[57]. Such media is needed to shift the myoblast and myotubes from glycolytic to oxidative metabolism that may lead to more mature forms of muscle tissue. Such changes may shift the balance of GLUT1 and GLUT4 expression to produce levels of these proteins that are closer to those occurring *in vivo*.

Methods are needed to control the development of fast and slow muscle fibers. The isolated myoblasts produce muscle fibers that represent the tissue biopsied[28, 91] does constrain the initial phenotype of the muscle, combinations of electrical stimulation, media conditions, and microRNAs could be used to bias differentiation. Optimization of contractile force has been one approach [40], but focusing on other properties of muscle (e.g. contraction velocity, calcium dynamics) could shift fiber type. However, developing myobundles of predominately type I or type II fibers would provide helpful in studying these fiber types under different environmental conditions.

The potential for 3D muscle models to facilitate therapies has been established with muscular dystrophy. Additional diseases to study include glycogen storage diseases, cachexia, neuromuscular disease and sarcopenia. Neuromuscular junctions have been developed in 2D and 3D systems and optogenetic stimulation is a promising approach to stimulate the neurons, results to date have merely established proof-of-principle. Conditions for neural innervation and stimulation of muscle needs to be optimized, and models need to be established for various neuromuscular diseases, such as myasthenia gravis, aging, and amyotrophic lateral sclerosis. Such models could advance the field and open new avenues to treat these debilitating diseases.

Acknowledgements

References

1. Baron AD, Brechtel G, Wallace P and Edelman SV, Am J Physiol, 1988, 255, E769–E774. [PubMed: 3059816]

2. Tabebordbar M, Wang ET and Wagers AJ, Annual Review of Pathology: Mechanisms of Disease, 2013, 8, 441–475.

3. Querol L and Illa I, Current Opinion in Neurology, 2013, 26, 459–465. [PubMed: 23945282]

4. Dalle S, Rossmeislova L and Koppo K, Frontiers in Physiology, 2017, 8.

5. Hwang H, Bowen BP, Lefort N, Flynn CR, De Filippis EA, Roberts C, Smoke CC, Meyer C, Højlund K, Yi Z and Mandarino LJ, Diabetes, 2010, 59, 33–42. [PubMed: 19833877]

6. Willmann R, Possekel S, Dubach-Powell J, Meier T and Ruegg MA, Neuromuscular Disorders, 2009, 19, 241–249. [PubMed: 19217290]

7. Romanick M, Thompson LV and Brown-Borg HM, Biochimica et Biophysica Acta (BBA) - Molecular Basis of Disease, 2013, 1832, 1410–1420. [PubMed: 23523469]

8. Seok J, Warren HS, Cuenca AG, Mindrinos MN, Baker HV, Xu W, Richards DR, McDonald-Smith GP, Gao H, Hennessy L, Finnerty CC, López CM, Honari S, Moore EE, Minei JP, Cuschieri J, Bankey PE, Johnson JL, Sperry J, Nathens AB, Billiar TR, West MA, Jeschke MG, Klein MB, Gamelli RL, Gibran NS, Brownstein BH, Miller-Graziano C, Calvano SE, Mason PH, Cobb JP, Rahme LG, Lowry SF, Maier RV, Moldawer LL, Herndon DN, Davis RW, Xiao W, Tompkins RG, t. Inflammation and L. S. C. R. P. Host Response to Injury, Proceed Natl Acad Sci, 2013, 110, 3507–3512.

9. Yin H, Price F and Rudnicki MA, Physiol Rev, 2013, 93, 23–67. [PubMed: 23303905]

10. Juhas M, Ye J and Bursac N, Methods, 2016, 99, 81–90. [PubMed: 26455485]

11. Rando TA and Blau HM, The Journal of Cell Biology, 1994, 125, 1275–1287. [PubMed: 8207057]

12. Gawlitta D, Boonen KJ, Oomens CW, Baaijens FP and Bouten CV, Tissue Eng Part A, 2008, 14, 161–171. [PubMed: 18333814]

13. Vandenburgh H, Shansky J, Del Tatto M and Chromiak J, Methods Mol Med., 1999, 18, 217–225. [PubMed: 21370179]

14. Khodabukus A and Baar K, Cells Tissues Organs, 2015, 202, 159–168.

15. Khodabukus A and Baar K, Tissue Eng Part A, 2015, 21, 1003–1012. [PubMed: 25333771]

16. Dennis RG, Kosnik PE, Gilbert ME and Faulkner JA, American Journal of Physiology - Cell Physiology, 2001, 280, C288–C295. [PubMed: 11208523]

17. Dennis RG and Kosnik PE, In Vitro Cell Dev Biol Anim, 2000, 36, 327–335. [PubMed: 10937836]

18. Qazi TH, Mooney DJ, Pumberger M, Geißler S and Duda GN, Biomaterials, 2015, 53, 502–521. [PubMed: 25890747]

19. Gilbert PM, Havenstrite KL, Magnusson KEG, Sacco A, Leonardi NA, Kraft P, Nguyen NK, Thrun S, Lutolf MP and Blau HM, Science, 2010, 329, 1078–1081. [PubMed: 20647425]

20. Engler AJ, Griffin MA, Sen S, Bonnemann CG, Sweeney HL and Discher DE, J Cell Biol, 2004, 166, 877–887. [PubMed: 15364962]

21. Hinds S, Bian W, Dennis RG and Bursac N, Biomaterials, 2011, 32, 3575–3583. [PubMed: 21324402]

22. Salimath AS and García AJ, Journal of Tissue Engineering and Regenerative Medicine, 2016, 10, 967–976. [PubMed: 24616405]

23. Ahadian S, Ramón-Azcón J, Estili M, Liang X, Ostrovidov S, Shiku H, Ramalingam M, Nakajima K, Sakka Y, Bae H, Matsue T and Khademhosseini A, Scientific Reports, 2014, 4, 4271. [PubMed: 24642903]

24. Porras AM, Westlund JA, Evans AD and Masters KS, Proceedings of the National Academy of Sciences of the United States of America, 2018, 115, E363–E371 [PubMed: 29282325]

25. Rhim C, Lowell DA, Reedy MC, Slentz DH, Zhang SJ, Kraus WE and Truskey GA, Muscle Nerve, 2007, 36, 71–80. [PubMed: 17455272]

26. Bian W and Bursac N, Biomaterials, 2009, 30, 1401–1412. [PubMed: 19070360]

27. Khodabukus A, Baehr LM, Bodine SC and Baar K, Journal of Cellular Physiology, 2015, 230, 2489–2497. [PubMed: 25857846]

28. Khodabukus A and Baar K, Journal of Cellular Physiology, 2015, 230, 1750–1757. [PubMed: 25335966]

29. Powell CA, Smiley BL, Mills J and Vandenburgh HH, American Journal of Physiology - Cell Physiology, 2002, 283, C1557–C1565. [PubMed: 12372817]

30. Gholobova D, Decroix L, Van Muylder V, Desender L, Gerard M, Carpentier G, Vandenburgh H and Thorrez L, Tissue Eng Part A, 2015, 21, 2548–2558. [PubMed: 26177063]

31. Madden L, Juhas M, Kraus WE, Truskey GA and Bursac N, eLife, 2015, 4, e04885. [PubMed: 25575180]

32. Vandenburgh H, Shansky J, Benesch-Lee F, Barbata V, Reid J, Thorrez L, Valentini R and Crawford G, Muscle & Nerve, 2008, 37, 438–447. [PubMed: 18236465]

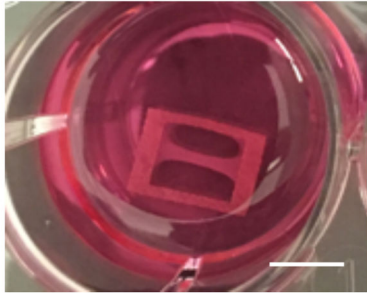33. Juhas M and Bursac N, Biomaterials, 2014, 35, 9438–9446. [PubMed: 25154662]

34. Lee PHU and Vandenburgh HH, Tissue Eng Part A, 2013, 19, 2147–2155. [PubMed: 23574457]

35. Davis BNJ, Santoso J, Walker M, Koves T, Kraus W and Truskey G, Tissue Eng Part C, 2017, 23, 189–199.

36. Close R, Physiol Rev, 1972, 52, 129–197. [PubMed: 4256989]

37. Baker JS, McCormick MC and Robergs RA, J Nutrition Metab, 2010, 2010, 905612. [PubMed: 21188163]

38. Racca AW, Klaiman JM, Pioner JM, Cheng Y, Beck AE, Moussavi-Harami F, Bamshad MJ and Regnier M, The Journal of Physiology, 2016, 594, 437–452. [PubMed: 26460603]

39. Racca AW, Beck AE, Rao VS, Flint GV, Lundy SD, Born DE, Bamshad MJ and Regnier M, The Journal of Physiology, 2013, 591, 3049–3061. [PubMed: 23629510]

40. Juhas M, Engelmayr GC, Fontanella AN, Palmer GM and Bursac N, Proceedings of the National Academy of Sciences, 2014, 111, 5508–5513.

41. Shimizu K, Araki H, Sakata K, Tonomura W, Hashida M and Konishi S, Journal of Bioscience and Bioengineering, 2015, 119, 212–216. [PubMed: 25085533]

42. Legant WR, Pathak A, Yang MT, Deshpande VS, McMeeking RM and Chen CS, Proceedings of the National Academy of Sciences, 2009, 106, 10097–10102.

43. Sakar MS, Neal D, Boudou T, Borochin MA, Li Y, Weiss R, Kamm RD, Chen CS and Asada HH, Lab on a Chip, 2012, 12, 4976–4985. [PubMed: 22976544]

44. Collinsworth AM, Zhang S, Kraus WE and Truskey GA, American Journal of Physiology-Cell Physiology, 2002, 283, C1219–C1227. [PubMed: 12225985]

45. Agrawal G, Aung A and Varghese S, Lab on a Chip, 2017, 17, 3447–3461. [PubMed: 28871305]

46. Khodabukus A and Baar K, Tissue Eng Part C, 2012, 18, 349–357.

47. Donnelly K, Khodabukus A, Philp A, Deldicque L, Dennis RG and Baar K, Tissue Eng Part C: Methods, 2010, 16, 711–718. [PubMed: 19807268]

48. Asano T, Ishizua T and Yawo H, Biotechnol Bioeng, 2012, 109, 199–204. [PubMed: 21809334]

49. Raman R, Cvetkovic C, Uzel SGM, Platt RJ, Sengupta P, Kamm RD and Bashir R, Proceedings of the National Academy of Sciences, 2016, 113, 3497–3502.

50. Park S-J, Gazzola M, Park KS, Park S, Di Santo V, Blevins EL, Lind JU, Campbell PH, Dauth S, Capulli AK, Pasqualini FS, Ahn S, Cho A, Yuan H, Maoz BM, Vijaykumar R, Choi J-W, Deisseroth K, Lauder GV, Mahadevan L and Parker KK, Science, 2016, 353, 158–162. [PubMed: 27387948]

51. Alford PW, Feinberg AW, Sheehy SP and Parker KK, Biomaterials, 2010, 31, 3613–3621. [PubMed: 20149449]

52. Wilson K, Das M, Wahl KJ, Colton RJ and Hickman J, PLoS One, 2010, 5, e11042. [PubMed: 20548775]

53. Feinberg AW, Feigel A, Shevkoplyas SS, Sheehy S, Whitesides GM and Parker KK, Science, 2007, 317, 1366–1370. [PubMed: 17823347]

54. Agarwal A, Goss JA, Cho A, McCain ML and Parker KK, Lab on a Chip, 2013, 13, 3599–3608. [PubMed: 23807141]

55. Nawroth JC, Scudder LL, Halvorson RT, Tresback J, Ferrier JP, Sheehy SP, Cho A, Kannan S, Sunyovszki I, Goss JA, Campbell PH and Parker KK, Biofabrication, 2018, 10, 025004. [PubMed: 29337695]

56. Pirozzi KL, Long CJ, McAleer CW, Smith AST and Hickman JJ, Applied Physics Letters, 2013, 103, 083108.

57. Smith A, Long C, Pirozzi K, Najjar S, McAleer C, Vandenburgh H and Hickman J, Journal of Biotechnology, 2014, 185, 15–18. [PubMed: 24909944]

58. Rao L, Qian Y, Khodabukus A, Ribar T and Bursac N, Nature Communications, 2018, 9, 126.

59. Maffioletti SM, Sarcar S, Henderson ABH, Mannhardt I, Pinton L, Moyle LA, Steele-Stallard H, Cappellari O, Wells KE, Ferrari G, Mitchell JS, Tyzack GE, Kotiadis VN, Khedr M, Ragazzi M, Wang W, Duchen MR, Patani R, Zammit PS, Wells DJ, Eschenhagen T and Tedesco FS, Cell Reports, 2018, 23, 899–908. [PubMed: 29669293]

60. Iovino S, Burkart AM, Warren L, Patti ME and Kahn CR, Proceedings of the National Academy of Sciences of the United States of America, 2016, 113, 1889–1894. [PubMed: 26831110]

61. Chal J, Al Tanoury Z, Hestin M, Gobert B, Aivio S, Hick A, Cherrier T, Nesmith AP, Parker KK and Pourquié O, Nature Protocols, 2016, 11, 1833. [PubMed: 27583644]

62. Chal J and Pourquie O, Development, 2017, 144, 2104–2122. [PubMed: 28634270]

63. Choi J, Costa ML, Mermelstein CS, Chagas C, Holtzer S and Holtzer H, Proceedings of the National Academy of Sciences, 1990, 87, 7988–7992.

64. Manandhar D, Song L, Kabadi A, Kwon JB, Edsall LE, Ehrlich M, Tsumagari K, Gersbach CA, Crawford GE and Gordân R, Nucleic Acids Research, 2017, 45, 11684–11699. [PubMed: 28977539]

65. Boularaoui SM, Abdel-Raouf KMA, Alwahab NSA, Kondash ME, Truskey GA, Teo JCM and Christoforou N, Journal of Tissue Engineering and Regenerative Medicine, 2018, 12, e918–e936. [PubMed: 28101909]

66. Wakao J, Kishida T, Fumino S, Kimura K, Yamamoto K, Kotani S.-i., Mizushima K, Naito Y, Yoshikawa T, Tajiri T and Mazda O, Biochemical and Biophysical Research Communications, 2017, 488, 368–373. [PubMed: 28501623]

67. Midrio M, European Journal of Applied Physiology, 2006, 98, 1–21. [PubMed: 16896733]

68. Bian W and Bursac N, FASEB Journal, 2012, 26, 955–965. [PubMed: 22075647]

69. Larkin LM, Van der Meulen JH, Dennis RG and Kennedy JB, In Vitro Cell Dev Biol Anim 2006, 42.

70. Martin NR, Passey SL, Player DJ, Mudera V, Baar K, Greensmith L and Lewis MP, Tissue Eng Part A, 2015, 21, 2595–2604. [PubMed: 26166548]

71. Morimoto Y, Kato-Negishi M, Onoe H and Takeuchi S, Biomaterials, 2013, 34, 9413–9419. [PubMed: 24041425]

72. Smith AST, Long CJ, Pirozzi K and Hickman JJ, Technology (Singap World Sci), 2013, 1, 37–48. [PubMed: 25019094]

73. Park JW, Vahidi B, Taylor AM, Rhee SW and Jeon NL, Nature Protocols, 2006, 1, 2128. [PubMed: 17487204]

74. Santhanam N, Kumanchik L, Guo X, Sommerhage F, Cai Y, Jackson M, Martin C, Saad G, McAleer CW, Wang Y, Lavado A, Long CJ and Hickman JJ, Biomaterials, 2018, 166, 64–78. [PubMed: 29547745]

75. Uzel SGM, Platt RJ, Subramanian V, Pearl TM, Rowlands CJ, Chan V, Boyer LA, So PTC and Kamm RD, Science Advances, 2016, 2, e1501429. [PubMed: 27493991]

76. Bonadonna RC, Groop L, Kraemer N, Ferrannini E, Del Prato S and DeFronzo RA, Metabolism: Clinical and Experimental, 1990, 39, 452–459. [PubMed: 2186255]

77. DeFronzo RA, Jacot E, Jequier E, Maeder E, Wahren J and Felber JP, Diabetes, 1981, 30, 1000–1007. [PubMed: 7030826]

78. Al-Khalili L, Chibalin AV, Kannisto K, Zhang BB, Permert J, Holman GD, Ehrenborg E, Ding VD, Zierath JR and Krook A, Cellular and Molecular Life Sciences : CMLS, 2003, 60, 991–998. [PubMed: 12827286]

79. Ciaraldi TP, Abrams L, Nikoulina S, Mudaliar S and Henry RR, The Journal of Clinical Investigation, 1995, 96, 2820–2827. [PubMed: 8675652]

80. Ciaraldi TP, Phillips SA, Carter L, Aroda V, Mudaliar S and Henry RR, The Journal of Clinical Endocrinology and Metabolism, 2005, 90, 5551–5558. [PubMed: 16030168]

81. Henry RR, Abrams L, Nikoulina S and Ciaraldi TP, Diabetes, 1995, 44, 936–946. [PubMed: 7622000]

82. Sarabia V, Lam L, Burdett E, Leiter LA and Klip A, The Journal of Clinical Investigation, 1992, 90, 1386–1395. [PubMed: 1401073]

83. Sarabia V, Ramlal T and Klip A, Biochemistry and Cell Biology = Biochimie et Biologie Cellulaire, 1990, 68, 536–542. [PubMed: 2188683]

84. Stuart CA, Wen G, Gustafson WC and Thompson EA, Metabolism: clinical and experimental, 2000, 49, 1604–1609. [PubMed: 11145124]

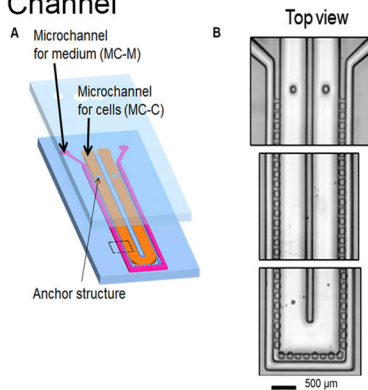85. Baker EL, Dennis RG and Larkin LM, In Vitro Cell Dev Biol Anim, 2003, 39, 434–439. [PubMed: 14741039]

86. Khodabukus A and Baar K, Journal of Cellular Physiology, 2015, 230, 1226–1234. [PubMed: 25358470]

87. Turner MC, Player DJ, Martin NRW, Akam EC and Lewis MP, Journal of Cellular Biochemistry, 2018, 119, 5686–5695. [PubMed: 29384221]

88. Syverud BC, Mycek M-A and Larkin LM Tissue Engineering Part C: Methods, 2017, 23, 616–626. [PubMed: 28810820]

89. Schiaffino S and Reggiani C, Physiol Rev, 2011, 91, 1447–1531. [PubMed: 22013216]

90. Bloemberg D and Quadrilatero J, PLoS One, 2012, 7, e35273. [PubMed: 22530000]

91. Huang Y-C, Dennis RG and Baar K, American Journal of Physiology-Cell Physiology, 2006, 291, C11–C17. [PubMed: 16436474]

92. Cheng CS, Ran L, Bursac N, Kraus WE and Truskey GA, Tissue Eng Part A, 2016, 22, 573–583. doi: 10.1089/ten.TEA.2015.0359. [PubMed: 26891613]

93. Heher P, Maleiner B, Prüller J, Teuschl AH, Kollmitzer J, Monforte X, Wolbank S, Redl H, Rünzler D and Fuchs C, Acta Biomaterialia, 2015, 24, 251–265. [PubMed: 26141153]

94. Vincent F, Loria P, Pregel M, Stanton R, Kitching L, Nocka K, Doyonnas R, Steppan C, Gilbert A, Schroeter T and Peakman M-C, Science Translational Medicine, 2015, 7, 293ps215.

95. Staffa JA, Chang J and Green L, The New England Journal of Medicine, 2002, 346, 539–540.

96. Pasnoor M and Dimachkie MM, Neurol Clin, 2014, 32, 647–670. [PubMed: 25037083]

97. Roden DM, The New England Journal of Medicine, 2004, 350, 1013–1022. [PubMed: 14999113]

98. Ju M and Wray D, FEBS letters, 2002, 524, 204–210. [PubMed: 12135768]

99. Vernetti L, Gough A, Baetz N, Blutt S, Broughman JR, Brown JA, Foulke-Abel J, Hasan N, In J, Kelly E, Kovbasnjuk O, Repper J, Senutovitch N, Stabb J, Yeung C, Zachos NC, Donowitz M, Estes M, Himmelfarb J, Truskey G, Wikswo JP and Taylor DL, Scientific Reports, 2017, 7, 42296. [PubMed: 28176881]

100. Zhang X, Hong S, Yen R, Kondash M, Fernandez C and Truskey GA, Lab on a Chip, 2018, (In Press).

101. Horvath P, Aulner N, Bickle M, Davies AM, Nery ED, Ebner D, Montoya MC, Östling P, Pietiäinen V, Price LS, Shorte SL, Turcatti G, von Schantz C and Carragher NO, Nature Reviews Drug Discovery, 2016, 15, 751. [PubMed: 27616293]

102. Jones DS, Jenney AP, Joughin BA, Sorger PK and Lauffenburger DA, Science Signaling, 2018, 11.

103. Schakman O, Kalista S, Barbé C, Loumaye A and Thissen JP, The International Journal of Biochemistry & Cell Biology, 2013, 45, 2163–2172. [PubMed: 23806868]

104. Shimizu K, Genma R, Gotou Y, Nagasaka S and Honda H, Bioengineering, 2017, 4, 56.

105. Syverud BC, VanDussen KW and Larkin LM, Tissue Eng Part A, 2016, 22, 480–489. [PubMed: 26790477]

106. Flanigan KM, Neurologic Clinics, 2014, 32, 671–688. [PubMed: 25037084]

107. Koenig M, Hoffman EP, Bertelson CJ, Monaco AP, Feener C and Kunkel LM, Cell, 1987, 50, 509–517. [PubMed: 3607877]

108. Long C, Li H, Tiburcy M, Rodriguez-Caycedo C, Kyrychenko V, Zhou H, Zhang Y, Min Y-L, Shelton JM, Mammen PPA, Liaw NY, Zimmermann W-H, Bassel-Duby R, Schneider JW and Olson EN, Science Advances, 2018, 4.

109. Nesmith AP, Wagner MA, Pasqualini FS, O'Connor BB, Pincus MJ, August PRand Parker KK, The Journal of Cell Biology, 2016, 215, 47–56. [PubMed: 27697929]

110. Lee J, Echigoya Y, Duddy W, Saito T, Aoki Y, Takeda S. i. and Yokota T, PLOS ONE, 2018, 13, e0197084. [PubMed: 29771942]

111. Martin NR, Passey SL, Player DJ, Khodabukus A, Ferguson RA, Sharples AP, Mudera V, Baar K and Lewis MP, Biomaterials, 2013, 34, 5759–5765. [PubMed: 23643182]
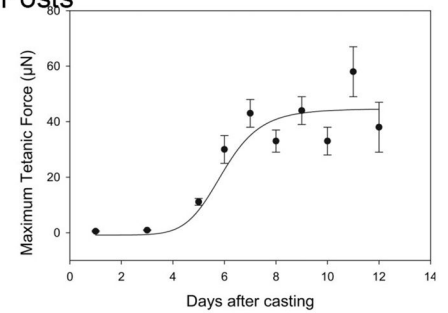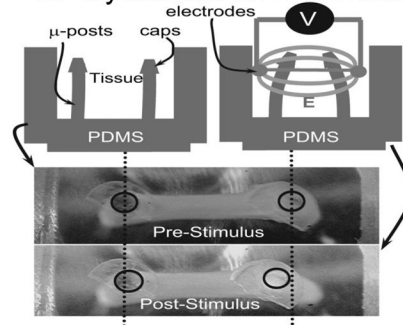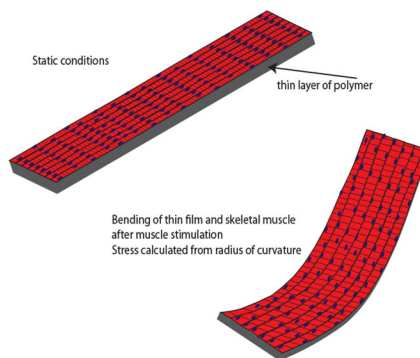
A. Myobundle on Fixed Frame
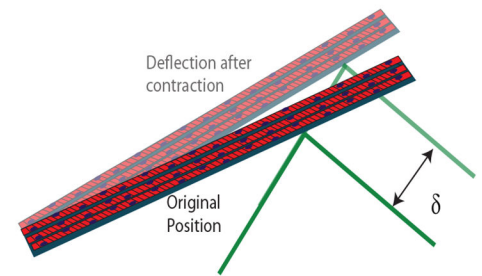
C. Myobundle on Deformable Posts

B. Myobundle in Microfluidic Channel

## D. Thin Muscular Film

E. Myotubes on Cantilever

Figure 1.
Overview of major types of skeletal muscle microphysiological systems. (**A**) A skeletal muscle myobundle fabricated with human myoblasts in a fibrin gel attached to a porous nylon frame as in Madden et al.[31] (Photo courtesy of Ringo Yen). (**B**) Left panel shows a schematic of the microfluidic channel to fabricate and perfuse myobundles[41]. The device consists of consists of an inner hairpin microchannel to prepare skeletal muscle collagen gel myobundles less than 100 mm thick and an outer hairpin channel for the culture media. Posts enable attachment and compaction of collagen gel, allowing orientation of myotubes. (From Shimizu et al.[41] with permission from Elsevier). (**C**) Aligned myofibers within myobundle attached to deformable posts, showing post deformation of the posts after electrical stimulation. Right panel shows the maturation of the tetanus force over time since fabrication (From Vandenburgh et al.[32] with permission from John Wiley and Sons). (**C**) Schematic of thin muscular films containing a uniform layer of skeletal myotubes. Aligned myotubes are produced by microcontact printing of extracellular matrix on the deformable polymer[107]. Contraction of the skeletal muscle cells following electrical or optogenetic stimulation causes bending of the myotubes and underlying polymer and the radius of curvature can be related to force. (**D**) Schematic of the deflection of a cantilever beam induced by contraction of one or more skeletal muscle myotubes attached to the cantilever. The cantilever deflection is measured by the displacement of a laser light that bounces off the cantilever.
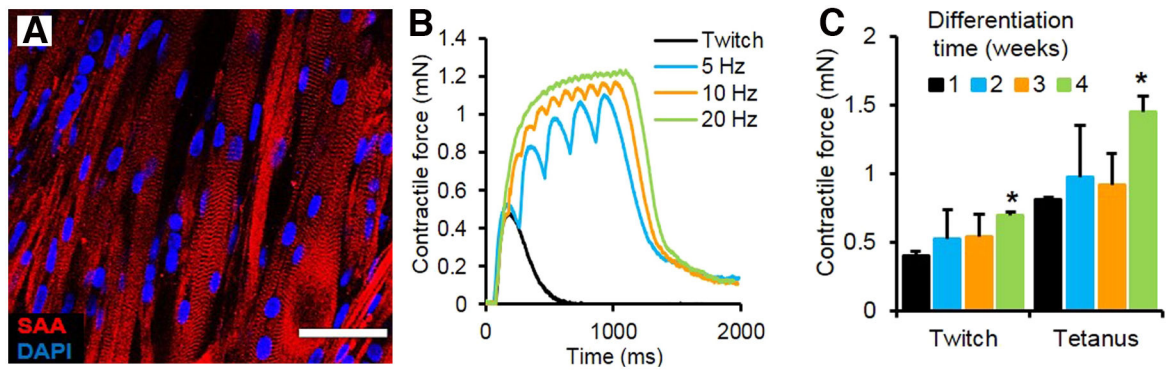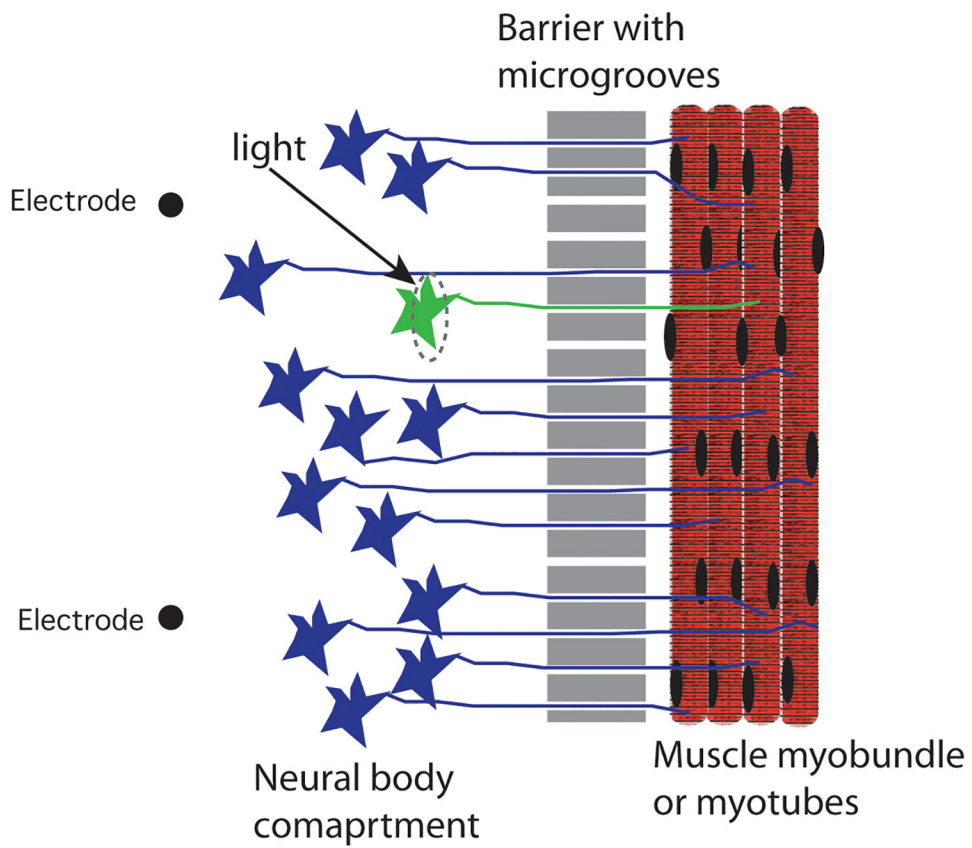
Figure 2.
(**A**) Aligned myofibers within myobundle exhibiting a striated pattern of the contractile protein sarcomeric α-actinin (SAA). (**B**) Representative contractile force traces of a 3-week myobundle showing fusion of individual twitches into a stronger tetanic contraction induced by increased stimulation frequency. (**C**) Twitch and tetanus forces increase over time in culture with significant enhancement at 4 weeks vs 1 week (*p < 0.05, n = 4 myobundles). From Madden et al.[31] and used per a Creative Common license http://creativecommons.org/licenses/by/4.0/.
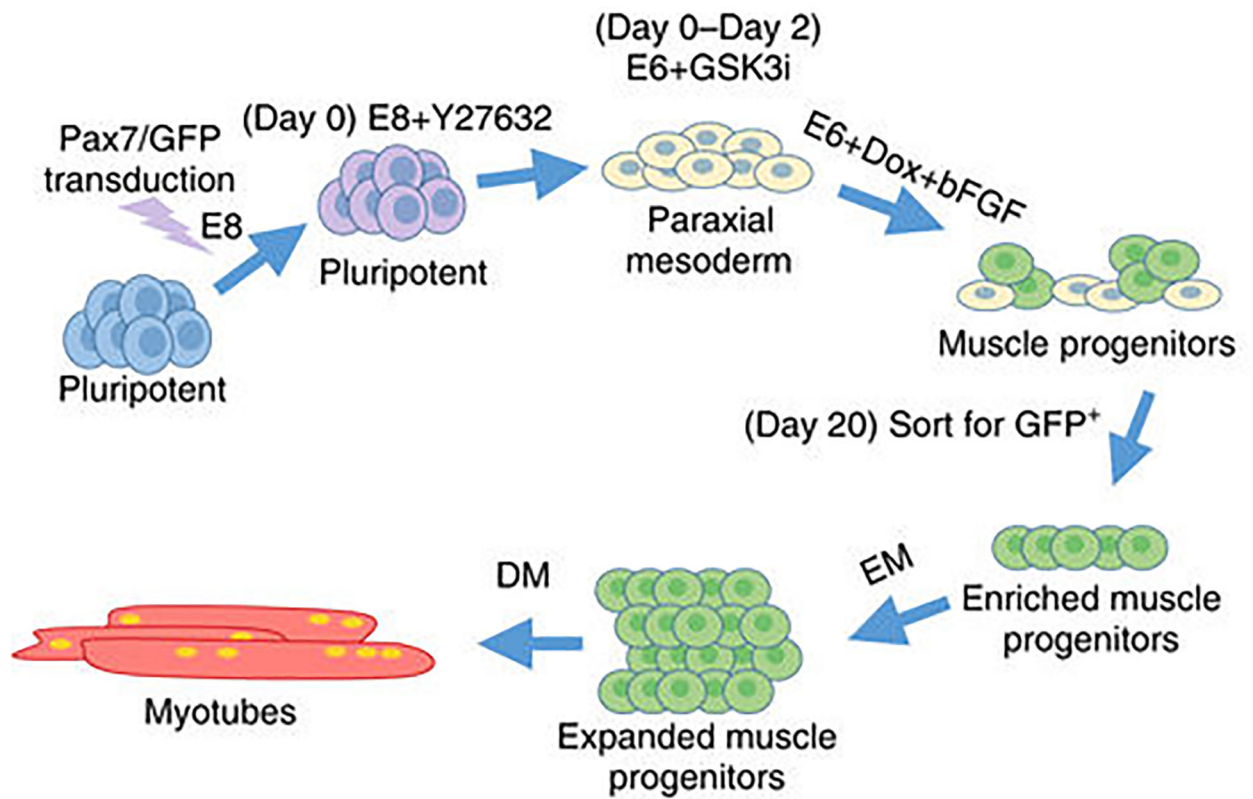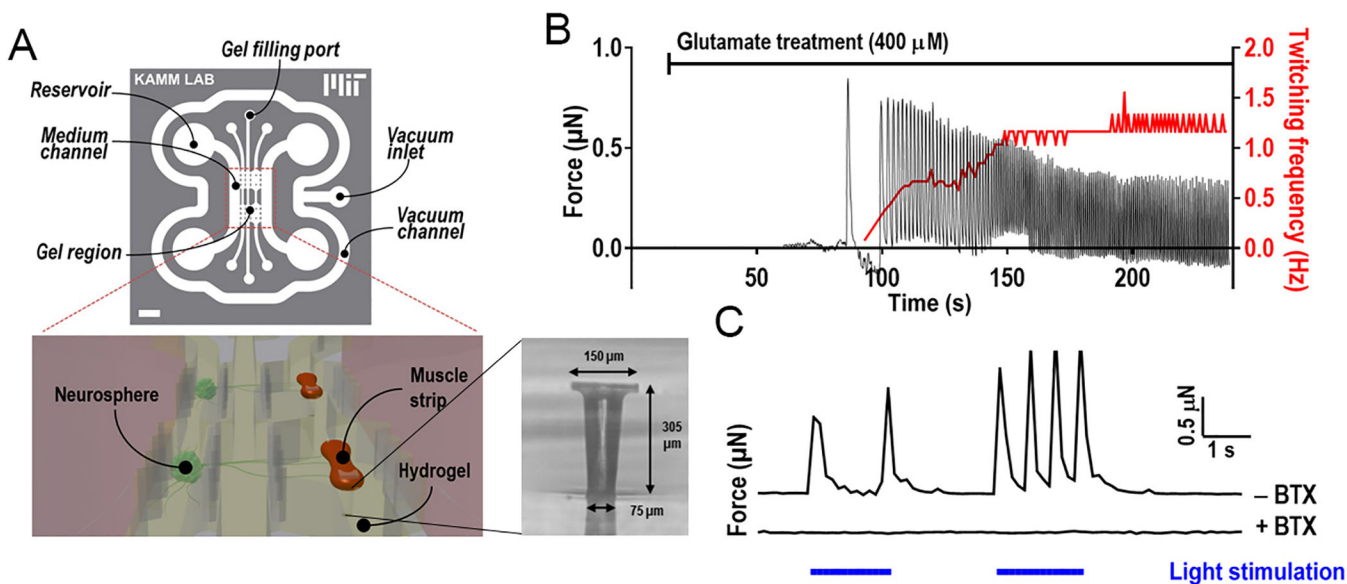
Figure 3.
Schematic of the process to produce Pax7+ induced myogenic precursor cells (iMPCs) and formation of myotubes. Dox represents doxycycline, EM represents expansion media, and DM represents differentiation media. From Rao et al. [56] and used per a Creative Common license http://creativecommons.org/licenses/by/4.0/.

Barrier with microgrooves

light

Electrode ●

Electrode ●

Neural body comaprtment

Muscle myobundle or myotubes

Figure 4.
Schematic of microfluidic chamber to allow motor neuron axons to attach to skeletal myotubes in 2D or 3D arrangements. The microgrooves allow single axons to grow and move in a directed manner towards the myotubes. Localized optogenetic stimulation of the green neuron and axon produces localized muscle contraction.
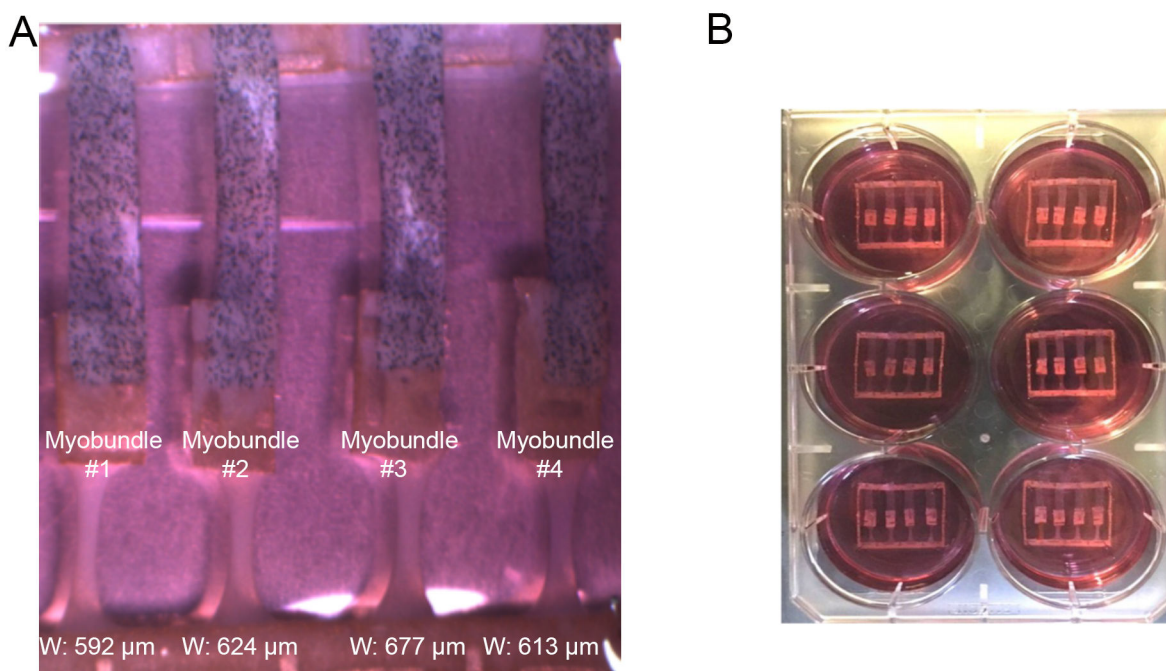
Figure 5.

(**A**) The microfluidic chamber for optogenetic stimulation of nerve and muscle consists of three parallel gel regions. The platform is composed of a top microfluidic layer assembled on top of a PDMS membrane featuring two sets of two capped pillars (inset), itself bonded to a coverslip. The two medium channels enable perfusion of nutrients and drugs. The vacuum channel enables the bonding of the microfluidic layer and pillar layer to the coverslip. Lower panels: Schematic of muscle bundles in a hydrogel innervated by neurospheres located in the opposite gel chamber separated by a 1-mm-wide gel region. Muscle bundles are attached to the two micropillars and contractile forces deflect pillars. (**B**) Application of glutamate to the medium results in a delayed stimulation of the muscle, leading to the initiation of muscle twitching with force at an increasing frequency (right *y* axis) as glutamate diffuses within the neurospheres. (**C**) Force generated by the muscle bundle upon illumination of the ChR2^{H134R}-HBG3-MN neurospheres on day 15. Application of αBTX inhibited the contractions. From Uzel et al. and used per a Creative Common license http://creativecommons.org/licenses/by/4.0/.
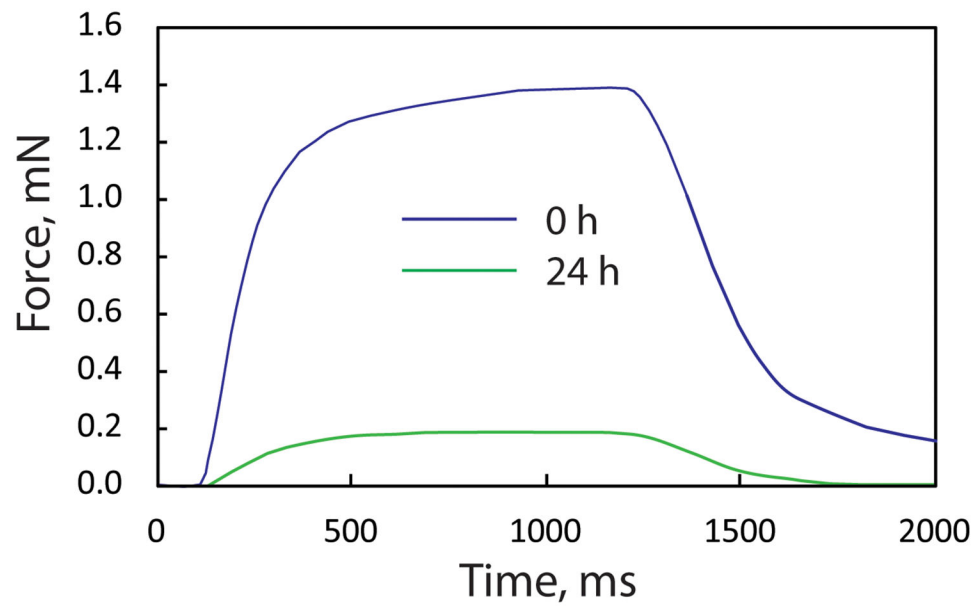
Figure 6.
Effect of 24 h exposure to 10 μM terfenadine on the tetanus force of myobundles in the arrangement show in Figure 1A. The blue curve represents the myobundle force occurring during a 0.8 s electrical stimulation at 20 Hz at the time of application of terfenadine and the green curve represents the tetanus force after 24 h exposure to 10 μM terfenadine. Exposure to the DMSO vehicle in which terfenadine was dissolved did not affect the tetanus force (unpublished results).

Figure 7.
A. Expanded view of 4 myobundles attached each to an elastic membrane with embedded microparticles that serves as a force transducer for individual myobundles. B. A six well dish with each dish containing a nylon frame with 4 myobundles each attached to an elastic membrane. Adapted from Ref. 100 with permission from The Royal Society of Chemistry.

Table 1.

Skeletal Muscle Microphysiological Systems

Type of system	Strengths	Limitations	References
Myobundle in hydrogel attached to fixed ends	Measure twitch, tetanus, fatigue, and can undergo electrical stimulation; Can generate high specific forces; measure force-length relations and passive forces	Hydrogel ECM represents a higher volume fraction than *in vivo*. Myotube length much length than total myobundle length.	13, 15, 25 – 31, 33–35, 40
Scaffold-free myobundles	Produce high cell density	Absence of extracellular matrix limits contractile stress	16, 17
Microchannel myobundles	Small scale and microfluidic integration may facilitate scaleup	No direct measurement of force yet	41,
Myobundles attached to deformable posts	Enables higher throughout; Optogentic stimulation eliminates problems with electrical stimulation; generate biobots	Not all myofibers are stimulated optically; cannot perform force-length or passive force measurements.	32, 42, 43, 45, 48, 49, 50, 104
Thin muscular film	Can run at moderate throughput; Direct measure of contractile force	Generally, a 2D system; cannot measure passive forces or force-length relations	51–55, 109
Myotubes on cantilever	Measure contractile force on individual fibers	Difficult to assess interactions among myofibers; cannot measure passive forces or force-length relations	52, 56, 57, 72, 74